Published in final edited form as:
*J Mol Biol*. 2006 December 1; 364(3): 302–308.

# DBC2 is Essential for Transporting Vesicular Stomatitis Virus Glycoprotein

**Faith K. Chang**[1,2], **Noriko Sato**[3], **Noriko Kobayashi-Simorowski**[1], **Takashi Yoshihara**[1], **Jennifer L. Meth**[2], and **Masaaki Hamaguchi**[1,*]

1 *Department of Biological Sciences, Fordham University, 441 E Fordham Road, Bronx, NY 10458*

2 *Cold Spring Harbor Laboratory, 1 Bungtown Road, Cold Spring Harbor, NY 11724*

3 *Cytokine project, Tokyo Metropolitan Institute of Medical Science, 3-18-22, Honkomagome, Bunkyo-ku, Tokyo 113-8613, Japan*

## Summary

DBC2 is a tumor suppressor gene linked to breast and lung cancers. Although DBC2 belongs to the RHO GTPase family, it has a unique structure that contains a Broad-Complex/Tramtrack/Bric a Brac (BTB) domain at the C terminus instead of a typical CAAX motif. A limited number of functional studies on DBC2 have indicated its participation in diverse cellular activities such as ubiquitination, cell cycle control, cytoskeleton organization and protein transport. In this paper, DBC2's role in protein transport was analyzed using vesicular stomatitis virus glycoprotein (VSVG) fused with green fluorescent protein (GFP). We discovered that DBC2 knockdown hinders the VSVG transport system in 293 cells. Previous literature demonstrates that VSVG is transported via the microtubule motor complex. We demonstrate that DBC2 mobility also depends on an intact microtubule network. We conclude that DBC2 plays an essential role in microtubule-mediated VSVG transport from ER to Golgi apparatus.

### Keywords

DBC2; protein transport; VSVG ts045; fluorescence microscope; FRAP

## Introduction

DBC2 is a tumor suppressor gene involved in breast cancer development. It is inactivated in more than half of breast cancer specimens and demonstrated to suppress breast cancer cell growth. Deduced amino acid sequence revealed that DBC2 contains well-conserved RAS and BTB/POZ (Broad-Complex Tramtrack Bric a Brac/Poxvirus Zinc Finger) domains that classify DBC2 as a member of the RHOBTB family. The RAS domain of DBC2 has high homology to that of small GTP-binding proteins (G-proteins), including the sites for binding to and hydrolysis of GTP. However, DBC2 is distinct from the typical RAS family member. DBC2 lacks the carboxyl terminal CAAX motif that is essential for isoprenylation, indicating a different role for DBC2 in association with the membrane. DBC2 has BTB domains in the middle of its structure, which makes DBC2 markedly bigger than most G-proteins. The unique structure of DBC2 suggests that it may be functionally divergent from canonical G proteins.

Although RHOBTB is an evolutionarily conserved protein with homologs in *Mus musculus* and *Drosophila Melanogaster*, homologs are not found in all eukaryotes and are remarkably

* Corresponding author: Department of Biological Sciences, Fordham University, 441 E Fordham Road, Larkin Hall, Bronx, NY 10458, Tel: (718) 817-3656, Fax: (718) 817-3645, e-mail: hamaguchi@fordham.edu.

absent in *Caenorhabditis elegans* and *Saccharomyces cerevisiae*[1]. RHOBTB is also found in non-mammals such as RacA of *Dictyostelium discoideum.* However, mammalian RHOBTB proteins and *Dictyostelium* RacA have considerable differences[2]. One of the more important distinctions involves the critical residues for GTPase activity that are conserved in RacA but not in human RHOBTB (for example, codons 86 and 88 of DBC2). We demonstrate that DBC2 does not bind to GTP in this paper. Since proteins with GTPase activity are likely to play a discrete role from those without GTPase activity, mammalian RHOBTB may very well have a different evolutionary origin from that of *Dictyostelium* RacA. Indeed, the absence of RHOBTB in *C. elegans* suggests that the mammalian RHOBTB emerged recently in the evolutionary stage. As for DBC2, the orthologous genes are found only in mammals, implying that DBC2 function may be related to the higher orchestration of cellular activity. This can only be elucidated by studying mammalian genes.

The Ras superfamily comprises five branches: Ras, Rho, Rab, Ran and Arf families. Each branch contains GTPases that function as molecular switches in a wide variety of cellular pathways[3]. GTPases bounce between active and inactive states as one binds to GTP and the other to GDP, respectively. This GTP/GDP cycling is controlled by three types of regulatory proteins - Guanine nucleotide exchange factors (GEFs), GTPase-activating proteins (GAPs) and Guanine nucleotide dissociation inhibitors (GDIs) – that frequently engage members of the Ras superfamily. The RHO (Ras homologous) proteins are known to play a key role in actin organization, microtubule dynamics, membrane trafficking and transcriptional regulation[4]. As a reflection of their involvement in such diverse cellular pathways, RHO GTPases interact with a motley collection of GAPs and GEFs and regulate similarly diverse downstream effectors. Rnd and RHOBTB are exceptional Rho proteins in that they have mutations at the crucial residues for hydrolysis of GTP. In fact, Rnd does not hydrolyze GTP *in vitro*, which implies that essential GAPs remain undiscovered or GAPs are controlled by transcriptional regulation and/or protein degradation[5; 6]. The number of target effectors for the three best characterized GTPases (RHOA, RAC1 and CDC42) exceeds 60 but few effectors for the other members of Rho GTPases have been identified. RHOBTB proteins including DBC2 have yet to be characterized and their regulatory proteins and effectors remain unknown.

The BTB/POZ domain is an evolutionarily conserved protein-protein interaction motif of approximately 115 amino acids[7]. Many BTB/POZ proteins are transcriptional regulators that mediate gene expression through the control of chromatin conformation. Such examples are BACH1, BACH2, PATZ and PLZF, all of which interact with other proteins through their BTB/POZ domains in a very specific manner. The interspecifically conserved residues within the BTB/POZ domain have been shown to be crucial for the interaction. Well-conserved, charged residues within the BTB/POZ domain are exposed into a pocket formed by the BTB/POZ domains of interacting proteins. Although the charged residues are not essential for oligomerization, they play a critical role in transcriptional regulation by the complex[8]. Other BTB/POZ proteins with Kelch repeats have been reported to bind to actins[9]. BTB/POZ proteins are demonstrated to recruit substrates for Cul3 ubiquitin ligases, suggesting RHOBTB's involvement in protein degradation pathways[10]. Their role as adapters requires specific recognition of the substrate that is bestowed by additional domains in some BTB/POZ proteins. DBC2 is shown to interact with Cul3 but its specific substrates have not been identified.

DBC2's novel combination of structural domains, lack of a membrane anchor sequence at the C-terminus and crucial mutation in the GTPase domain suggests that DBC2's function may not be deduced from other members of the RAS superfamily. Previous studies of RHOBTB have suggested several cellular functions. RhoBTB was found to suppress the overgrowth of *drosophila* larval neuromuscular synapse induced by *N*-ethylmaleimide sensitive factor (NSF)[11]. Although the authors surmised that RhoBTB is a potential regulator of the cytoskeleton, it is also possible that RhoBTB participates in other pathways that are relevant to the suppression

of NSF neuromuscular junction overgrowth, including the ubiquitin pathway and signal transduction. In fact, DBC2 interacts with ubiquitin ligase like other BTB proteins, indicating its involvement in the ubiquitin pathway[10]. Expression microarray analysis revealed that DBC2 alters expression levels of genes in charge of cell cycle control, apoptosis, cytoskeleton and membrane trafficking[12]. These findings infer that DBC2 participates in various cellular activities. As part of a comprehensive study on DBC2 function, DBC2's role in protein transport was investigated.

Fluorochromes allow real-time observation of protein movement in live cells and thorough analysis of subcellular localization of proteins. Additionally, manipulation of fluorescent signal facilitates the study of protein kinetics through techniques such as FRAP (fluorescence recovery after photobleaching) and FLIP (fluorescence loss in photobleaching). VSVG-EGFP (ts045), a well-characterized chimeric protein, has been utilized for a number of studies on protein transport. VSVG is transported from ER to Golgi by pre-Golgi structures along the microtubule tracks[13]. We demonstrate here that DBC2 knockdown severely incapacitates VSVG-EGFP (ts045) transport. Additionally, DBC2 transport depends on an intact microtubule network. These findings indicate that DBC2 plays a crucial role in VSVG transport in a microtubule dependent manner.

## Results

### GTP binding assay of DBC2

A GTP binding assay was carried out to confirm that mutations of the critical residues in the Ras domain (codons 86 and 88) make DBC2 non-functional as a GTPase. A truncated mutant containing only codons 1 through 160 and wild type DBC2 did not bind to GTP whereas p21 Ras bound to GTP (Figure 1). This result suggests that the Ras domain of DBC2, like that of Rnd, may play a distinctive role among Rho GTPases.

### Endogenous DBC2 expression in 293 cells

DBC2 expression level varies depending on the type of cell. Certain cells are led to growth arrest by exogenous DBC2 while others tolerate DBC2 [1]. In order to examine the expression level of endogenous DBC2 in 293 cells, DBC2 protein was stained with anti-DBC2 antibody N15 (Delta Labs). Expression of endogenous DBC2 was observed in the 293 cells (Figure 2). Furthermore, the 293 cells continued to grow after transformation with DBC2 expression vector. The different responses to DBC2 may be explained by the cellular dependency on a particular biological pathway discussed in the *Discussion* section. We concluded that 293 cells are suitable for functional analysis of DBC2 due to their property of expressing endogenous DBC2 and ability to withstand exogenous DBC2 overexpression.

### Kinetics of VSVG-EGFP (ts045) in 293 cells and SK-BR-3 cells

In order to verify the VSVG-EGFP (ts045) clone to be used in the experiments, its kinetics was examined in 293 and Sk-Br-3 cells. After transformation of 293 and SK-BR-3 cells, VSVG-EGFP (ts045) signal was mainly observed at the cellular membrane and Golgi apparatus during incubation at 37 °C (Figure 3a). VSVG-EGFP (ts045) is known to stay within the ER at a higher temperature due to a reversible abnormal folding[13]. This was confirmed by observing that the transformants at a nonpermissive temperature (39 °C) exhibited VSVG-EGFP (ts045) signal exclusively at the endoplasmic reticulum (ER) (Figure 3b). As the temperature was lowered to a permissive temperature (32 °C), the VSVG-EGFP (ts045) signal began to accumulate at the Golgi apparatus (Figure 3c). When a region of interest (ROI) was photobleached, the signal within the ROI recovered to more than 72% of the prebleached level within 60 seconds ($\sigma = 10$ %). These observations are concordant with published data of VSVG-EGFP (ts045) kinetics in COS and U2OS cells.[14; 15] We can reasonably assume that 293 and

SK-BR-3 cells transport VSVG-EGFP (ts045) in the same manner as well-characterized COS cells.

### DBC2's role in VSVG transport

In order to determine the role of DBC2 in VSVG transport, DBC2 was knocked down in 293 cells and the kinetics of VSVG-EGFP (ts045) was studied (293-KD). Control 293 cells (293-C) were prepared as described in the *Materials and Methods* section and analyzed alongside 293-KD cells. There was no noticeable difference in VSVG-EGFP (ts045) kinetics between 293-C and wild type 293 cells. The distribution of the fluorescent signal was observed at the cellular membrane and the Golgi apparatus. The recovery curve and the mobile fraction of VSVG-EGFP (ts045) in the 293-C cells were indistinguishable from those in the wild type 293 cells. In contrast, the recovery curve of VSVG-EGFP (ts045) in the 293-KD cells was markedly different from that in the 293-C cells. The mobile fraction significantly diminished to 22 % ($\sigma$ = 6.45%) ($p<0.01$) (Figure 4). In addition, VSVG-EGFP (ts045) in 293-KD cells was distributed in a distinct manner (Figure 5). The signal did not accumulate at the Golgi apparatus but intense signal was observed near the ER. Although signal was observed at the cellular membrane, it was ruggedly dispersed instead of neatly defined. VSVG-EGFP (ts045) modification at the Golgi apparatus was probably disrupted, which inhibited normal alignment of VSVG-EGFP (ts045) at the final destination. Two possible mechanisms are considered: (1) DBC2 facilitates the connection between VSVG and the microtubule cellular motor system. In this scenario, DBC2 knockdown would incapacitate efficient VSVG transport to the Golgi and subsequently lead to congregation of VSVG without posttranslational modification at the cellular membrane. (2) DBC2 is part of the tethering complex that connects VSVG to the pre-Golgi structure. Without DBC2, VSVG is not transported to nor accumulated at the Golgi apparatus. The export of VSVG from the ER is not affected by DBC2 knockdown, enabling VSVG to move freely by diffusion. The absence of signal accumulation at the Golgi may be explicated by the second hypothesis.

### Kinetics of GFP-DBC2 in 293 cells and SK-BR-3 cells

GFP-DBC2 signal in 293 and SK-BR-3 cells distributed homogenously throughout the cytoplasm when it was abundantly expressed. FRAP analysis revealed quick recovery of GFP-DBC2 signal (88 % in 20 seconds, $\sigma$ = 5.4 %) in 293 cells (Figure 4). Since RHO proteins bind to actin and participate in regulation of cytoskeletal dynamics, we investigated DBC2 kinetics after depolymerizing microtubules with 1 μM nocodazole. Although DBC2 distribution seemed unchanged, its movement, measured by FRAP analysis, was restricted ($p < 0.01$). After photobleaching the ROI, the fluorescent signal began to recover and reached a plateau in 20 seconds with 40 % signal recovery ($\sigma$ = 2.7 %) (Figure 4). We speculate that the initial recovery phase represents DBC2's free movement near the ROI. The lower recovery ratio and earlier saturation are caused by the inhibition of distant traveling, which indicates that an intact microtubule network is essential for long-range transport of DBC2. These findings also imply that free diffusion of DBC2 is restricted by binding to other proteins or saturation of DBC2 in the area. Indeed, immunocytochemical analysis demonstrated the localization of DBC2 alongside the microtubules (Figure 6). DBC2 distributed widely in the cytoplasm and did not appear to migrate heavily near particular organelles, unlike VSVG. This supports the hypothesis that DBC2 is a structural component of the tethering complex to the cellular motor system. Further experiments are needed to test this hypothesis.

## Discussion

We demonstrated that DBC2 plays a vital role in VSVG transport and depends upon an intact microtubule network to remain mobile. Previous publications established that the microtubule network is essential for VSVG transport[16]. However, there is still the crucial question of how

DBC2 participates in VSVG transport. There are several possible modes of action. (1) DBC2 is necessary for the export of VSVG from the ER. (2) DBC2 catalyzes the connection of VSVG to the cellular motor system. (3) DBC2 is a component of the structure that connects VSVG intermediate complex to the cellular motor system. VSVG-EGFP (ts045) is not confined in the ER even when DBC2 is knocked down, indicating that DBC2 is dispensable for export from the ER. Since GFP-DBC2 traveled in a microtubule dependent manner without losing fluorescent signal, at least a certain portion of DBC2 is likely to bind to the cellular motors directly or indirectly. This finding corroborates with previously published data that VSVG transport does not rely on vesicles [13]. In addition, DBC2 is actively transported even in the absence of VSVG-EGFP (ts045). These findings support the third mode of action (though the second mechanism remains possible) and incite several questions: Which proteins rely on DBC2 for connection to the cellular motor? Is DBC2's role limited to non-vesicular transportation? Does DBC2 bind to the cellular motor directly? If not, what other proteins compose the tethering system? These questions need to be addressed in future research.

Endogenous DBC2 was observed in the nucleus as well as the cytoplasm in some cells. The molecular weight of DBC2 is 83 kDa, exceeding the size limitation for free permeability (up to 9 nm, e.g. 40–60 kDa) into the nucleus. DBC2 has biological signatures that appear in nuclear proteins in the PROCITE database[17]. Interestingly, DBC2 does not have a known nuclear localization signal (NLS), which was confirmed by PredictNLS, an application that predicts NLS[18]. This discrepancy is not uncommon since only 43 % of the known nuclear proteins have matching NLS detectable by the PredictNLS. These findings indicate that DBC2 may be transported into the nucleus by an unknown nuclear transport system that recognizes uncharacterized motifs. Some nuclear G-proteins are transported between the nucleus and the cytoplasm. It is conceivable that DBC2 might shuttle in the same way.

SK-BR-3 and 293 cells are resistant to DBC2 expression despite DBC2's role as a tumor suppressor that works adversely in certain cells. Different responses to DBC2 may be caused by the nature of DBC2 sensitive cells that have become dependent on cellular pathways negatively regulated by DBC2. Many cellular pathways are redundant and the obstruction of signal transduction at a certain point is usually tolerated. However, some cancer cells have developed dependency on a particular cellular pathway, most commonly the oncogenic pathway. For example, *BCR-ABL* function has become vital in a subset of leukemia cells with a Philadelphia chromosome. Imatinib, a BCR-ABL inhibitor, works adversely in these cells, but does not severely damage other cells since they have alternatives to the ABL pathway.[19] Future experiments to test this hypothesis will include determining DBC2 sensitivity for a number of tumor cells and investigating the cellular pathways that involve DBC2 in these cells.

## Materials and Methods

### Reagents

All enzymes were supplied from New England Bio Labs (Beverly, MA) unless otherwise stated. Thermo-stable DNA polymerases were purchased from Applied Biosystems (Foster City, CA). Oligonucleotides were synthesized by Sigma Genosys (The Woodlands, TX). Rabbit anti-DBC2 polyclonal antibody (N15) was obtained from Delta Biolabs (Campbell, CA). Mouse monoclonal anti-rabbit IgG conjugated with TRITC was purchased from Santa Cruz Biotechnology (Santa Cruz, CA). HRP-conjugated anti-β actin antibody and anti-γ tubulin antibody were purchased from Sigma (St. Louis, MO). Alexa Fluor 568-conjugated goat anti-mouse IgG was purchased from Invitrogen (Carlsbad, CA). Guanosine 5′-[α-$^{32}$P] triphosphate, triethylammonium salt ([α-$^{32}$P] GTP) was purchased from Amersham (Piscataway, NJ)

## Cell culture

Cell culture reagents were purchased from Life Technologies (Gaithersburg, MD) unless otherwise stated. T47-D, SK-BR-3 (HTB-30), COS7 and 293 (CRL-1573) cells were obtained from American Tissue Type Collection (ATCC) and maintained in Dulbecco's Modified Eagle Medium (ICN Biomedicals Inc., Costa Mesa, CA) supplemented with 10 % FBS purchased from Atlas Biologicals (Fort Collins, CO) and antibiotics (50 units/ml penicillin and 50 μg/ml streptomycin) at 37 °C in a 5 % $CO_2$ incubator. Nocodazole was purchased from Sigma-Aldrich (St. Louis, MO).

## Constructs

Full-length cDNA of DBC2 was obtained from normal breast cDNA library, Soares 3NbHBst (the I.M.A.G.E. Consortium) and cloned into *Bam*HI-*Eco*RI sites of pCMV-tag2B plasmid (Stratagene, La Jolla, CA) to create pCMV-tag2B-DBC2. The entire insert was sequenced for both directions to verify the absence of mutations. The DBC2 ORF was inserted into the pEGFP-C1 vector to create GFP-DBC2 fusion protein (pEGFP-DBC2). The same ORF was cloned into pRSET-A vector to generate pRSET-DBC2. A truncated DBC2 ORF (nucleotides 1–480) was also inserted into pRSET-A vector so that the expressed protein would only contain a Ras domain (pRSET-DBC2-ΔBTB). VSVG-EGFP (ts045) construct was donated by Dr. Lippincott-Schwartz at NIH[13]. The constructs were transfected with Oligofectamine Reagent (Invitrogen, Carlsbad, CA) or FuGene6 (Roche, Indianapolis, IN), following the manufacturer's instructions.

## GTP binding Assay

Wild type and mutant DBC2 proteins were produced from pRSET-DBC2 and pRSET-DBC2-ΔBTB in an *E. coli* strain BL21 and subsequently purified with NiCAM HC resin (Sigma-Aldrich, St. Louis, MO). Ras protein was a gift from Dr. Linda Van Aelst. DBC2-ΔBTB (22kD), wt DBC2 (83 kD), Ras (positive control) and albumin (negative control) were analyzed through a 12 % SDS-PAGE. The proteins were transferred to a nitrocellulose membrane and submerged in a buffer (10mM $NaHCO_3$/ 3 mM $Na_2CO_3$, pH 9.8) for 15 minutes. The membrane was rinsed with a GTP binding buffer (50mM $NaH_2PO_4$, pH 7.5, 10 μM $MgCl_2$, 2mM DTT, 0.3% (v/v), Tween 20, 4 μM ATP) and then incubated in the GTP binding buffer containing 40m μCi [α-$^{32}$P] GTP (at 3000 Ci/mmol, 10 mCi/ml) for 2 hours at room temperature. After washing the membrane 6 times in the GTP binding buffer, autoradiography was performed for 15 hours.

## RNAi

Small interfering RNAs (siRNA) were purchased from Dharmacon Inc. (Lafeyette, CO). The siRNA sequences were DBC2-α: GAGAUGGCAGAAGAUCCUCdTdT, DBC2-β: CCAGGAGUAUUUCGAGAAGdTdT, and DBC2-γ: GACCGUCGCUUUGCUUAUGdTdT. Lamin siRNA was used as a control and supplied from Dharmacon Inc[12]. Target cells were transformed with siRNA at the concentration of 200 nM using Oligofectamine Reagent (Invitrogen, Carlsbad, CA), following manufacturer's instructions. The cells were then observed 24 hours after transformation. 293 cells with DBC2 knockdown (293-KD) and control 293 cells (293-C) were prepared side by side from the same progenitor cells to minimize biological artifacts. Both cells were treated with transformation reagents in the same manner except for the addition/subtraction of siRNAs: 293-KD with siRNAs for DBC2 and 293-C without siRNA. Effectiveness of siRNA was verified by immunocytochemistry.

## Microscope

All live cell imaging was performed using a Zeiss LSM 510 confocal microscope system (Carl Zeiss). Cells were plated on an acid-treated cover slide (0.17 mm thick) and then transformed with constructs of choice 24 hours prior to microscopic observation. The slide with cells was set in a Focht Chamber System 2 (FCS2) that was maintained at 37 °C. Confocal fluorescence images were acquired with a Zeiss Plan Apochromat (oil, 63x, 1.4 NA) objective and argon/krypton laser. For quantitative analysis, the pinhole was opened to collect fluorescence from the entire depth of the cell. The EGFP constructs were imaged with a filter set 44 (excitation: BP 475/40, beam splitter: FT500, emission: BP 530/50). Confocal fluorescence images were acquired with CLSM (Confocal Laser Scanning Microscopy Zeiss Axiovert 100). Collected images were analyzed with Carl Zeiss LSM software and converted to QuickTime movies. Single frame images were exported as TIFF files and processed with Photoshop CS for presentation. Measurements of fluorescence intensity within the ROI and whole cell were acquired by LSM software and exported to Microsoft Excel spread sheets for further calculation. For fluorescence recovery after photobleaching (FRAP), five images were taken before photobleaching at low laser intensity (< 1 %). The region of interest (ROI) was then scanned 6–10 times with the laser line at full laser power at zero attenuation. Immediately after photobleaching the cell, the fluorescence recovery within the ROI was monitored by time lapse imaging (4.98 s/frame) at low laser intensity (<1 %) unless otherwise stated. All experiments were repeated for at least 3 independent transformations. Each transformation was accompanied by controls with an empty vector transfection and unrelated construct.

## Immunocytology

For staining, all cells except COS7 cells were plated on 22 mm cover glass (0.17 mm thick) 24 hours prior to fixing. The cells were fixed by incubating in 4% paraformaldehyde for 10 minutes at room temperature and permeabilized by incubating in 0.5 % Triton X-100 and 0.1 % SDS in PBS for 5 minutes at room temperature. The specimens were then incubated in 10 % horse serum in PBS for 30 minutes at 37 °C. Antibody binding was performed in 1 % BSA in PBS. Rabbit anti-DBC2 antibody and mouse anti-rabbit IgG conjugated with FITC were used at 1/250 and 1/100 dilutions, respectively. Stained cells were observed with a TS100-F microscope (Nikon, Melville, NY) with CFI Plan Apochromat (oil, 60x, 1.4 NA) objective. Excitation light was obtained from T1-FM Epi Fluorescence Module through a HYQ-FITC filter (Ex 470/40, Dm 495, Bar 525/50). Images were captured with Insight-QE Color Digital camera and Act-2U Imaging Software. For immunocytochemical analysis of COS7 cells, pEGF-DBC2 plasmid was tranfected into COS7 cells using FuGene6 reagent. The cells were plated on a poly D-lysiene coated glass-bottom microwell dish (Mat Tek, MA) 6 hours after transformation. After 16 hours of incubation, cells were fixed with 2 % paraformaldehyde for 5 minutes and permeabilized with PBS containing 0.5 % Triton X-100 for 5 minutes. The specimens were incubated in a blocking buffer (4 % BSA and 0.1 % Tween 20 in PBS) for 30 minutes at 37 °C. The cells were then incubated in the blocking buffer containing anti α-tubulin. Alexa Fluor 568-conjugated goat anti-mouse IgG was used as a secondary antibody for immunofluorescence analysis. Nuclei were labeled with Hoechst 33342. The images were obtained with Olympus IX70 (Olympus, Center Valley, PA) and processed with a Deltavision Deconvolution Microscope (Applied Precision Inc. Issaquah, WA).

#### Acknowledgements

This work was supported by a grant from the National Institute of Health (1-R01-CA-100006-01) to MH. We are indebted to Stephen Hern and Carl Zeiss MicroImaging, Inc. for their help in microscopy. We acknowledge valuable support from Linda Van Aelst and Veeraiah Siripurapu in analyzing the RAS domain of DBC2. We thank Jennifer Lippincott-Schwartz for the VSVG-EGFP (ts045) and Yoshihiro Kitamura for critical scientific discussion.

## References


1. Hamaguchi M, Meth JL, Von Klitzing C, Wei W, Esposito D, Rodgers L, Walsh T, Welcsh P, King MC, Wigler MH. DBC2, a candidate for a tumor suppressor gene involved in breast cancer. Proc Natl Acad Sci U S A 2002;99:13647–13652. [PubMed: 12370419]
2. Rivero F, Dislich H, Glockner G, Noegel AA. The Dictyostelium discoideum family of Rho-related proteins. Nucleic Acids Res 2001;29:1068–79. [PubMed: 11222756]
3. Wennerberg K, Rossman KL, Der CJ. The Ras superfamily at a glance. J Cell Sci 2005;118:843–6. [PubMed: 15731001]
4. Etienne-Manneville S, Hall A. Rho GTPases in cell biology. Nature 2002;420:629–35. [PubMed: 12478284]
5. Chardin P. Function and regulation of Rnd proteins. Nat Rev Mol Cell Biol 2006;7:54–62. [PubMed: 16493413]
6. Nobes CD, Lauritzen I, Mattei MG, Paris S, Hall A, Chardin P. A new member of the Rho family, Rnd1, promotes disassembly of actin filament structures and loss of cell adhesion. J Cell Biol 1998;141:187–97. [PubMed: 9531558]
7. Collins T, Stone JR, Williams AJ. All in the family: the BTB/POZ, KRAB, and SCAN domains. Mol Cell Biol 2001;21:3609–15. [PubMed: 11340155]
8. Melnick A, Carlile G, Ahmad KF, Kiang CL, Corcoran C, Bardwell V, Prive GG, Licht JD. Critical residues within the BTB domain of PLZF and Bcl-6 modulate interaction with corepressors. Mol Cell Biol 2002;22:1804–18. [PubMed: 11865059]
9. Stogios PJ, Prive GG. The BACK domain in BTB-kelch proteins. Trends Biochem Sci 2004;29:634–7. [PubMed: 15544948]
10. Wilkins A, Ping Q, Carpenter CL. RhoBTB2 is a substrate of the mammalian Cul3 ubiquitin ligase complex. Genes Dev 2004;18:856–61. [PubMed: 15107402]
11. Laviolette MJ, Nunes P, Peyre JB, Aigaki T, Stewart BA. A genetic screen for suppressors of Drosophila NSF2 neuromuscular junction overgrowth. Genetics 2005;170:779–92. [PubMed: 15834148]
12. Siripurapu V, Meth JL, Kobayashi N, Hamaguchi M. DBC2 Significantly Influences Cell Cycle, Apoptosis, Cytoskeleton and Membrane Trafficking Pathways. J Molecular Biology. 2004in press
13. Presley JF, Cole NB, Schroer TA, Hirschberg K, Zaal KJ, Lippincott-Schwartz J. ER-to-Golgi transport visualized in living cells. Nature 1997;389:81–5. [PubMed: 9288971]
14. Dalal S, Rosser MF, Cyr DM, Hanson PI. Distinct roles for the AAA ATPases NSF and p97 in the secretory pathway. Mol Biol Cell 2004;15:637–48. [PubMed: 14617820]
15. Hirschberg K, Miller CM, Ellenberg J, Presley JF, Siggia ED, Phair RD, Lippincott-Schwartz J. Kinetic analysis of secretory protein traffic and characterization of golgi to plasma membrane transport intermediates in living cells. J Cell Biol 1998;143:1485–503. [PubMed: 9852146]
16. Presley JF, Smith C, Hirschberg K, Miller C, Cole NB, Zaal KJ, Lippincott-Schwartz J. Golgi membrane dynamics. Mol Biol Cell 1998;9:1617–26. [PubMed: 9658158]
17. Hulo N, Bairoch A, Bulliard V, Cerutti L, De Castro E, Langendijk-Genevaux PS, Pagni M, Sigrist CJ. The PROSITE database. Nucleic Acids Res 2006;34:D227–30. [PubMed: 16381852]
18. Cokol M, Nair R, Rost B. Finding nuclear localization signals. EMBO Rep 2000;1:411–5. [PubMed: 11258480]
19. Druker BJ, Sawyers CL, Kantarjian H, Resta DJ, Reese SF, Ford JM, Capdeville R, Talpaz M. Activity of a specific inhibitor of the BCR-ABL tyrosine kinase in the blast crisis of chronic myeloid leukemia and acute lymphoblastic leukemia with the Philadelphia chromosome. N Engl J Med 2001;344:1038–42. [PubMed: 11287973]

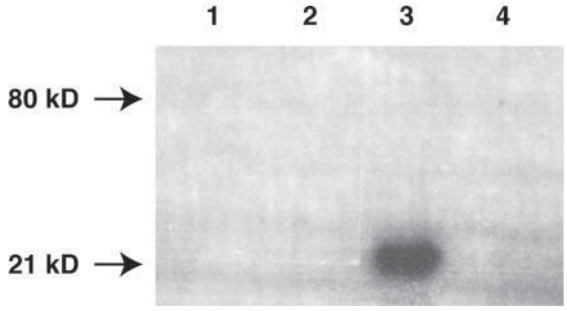


**Figure 1.**

GTP binding Assay. Lanes 1 through 4 contain 10 μg of truncated DBC2 (RAS domain only), 10 μg of wild type DBC2 protein, 4 μg of p21 Ras protein and 10 μg of albumin, respectively. Only lane 3 shows signal from [γ-32P] GTP. DBC2 is distinct from canonical Ras proteins in that it does not bind to GTP *in vitro*.

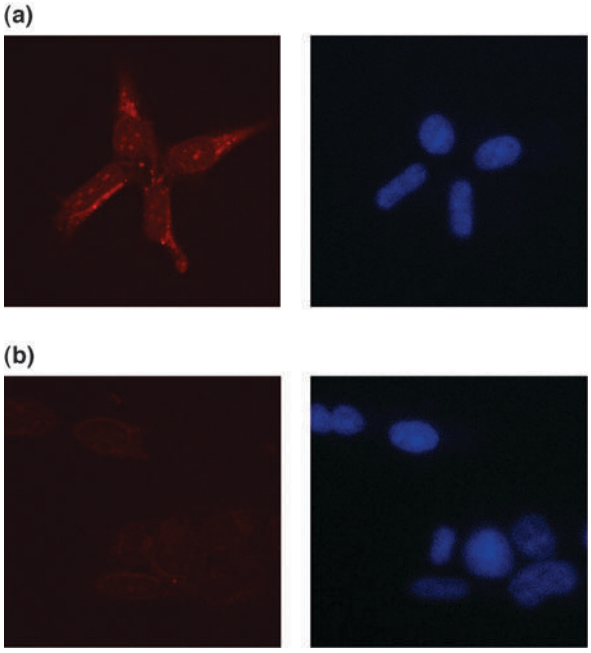


**Figure 2.**

Immunocytochemical analysis of 293 cells. *(a)* The left panel demonstrates wild type 293 cells. The specimen was incubated with rabbit anti-DBC2 antibody and then with mouse anti-rabbit antibody conjugated with TRITC. A counter stain of nuclei with DAPI is shown in the right. *(b)* The left panel shows 293 cells with DBC2 knockdown by RNAi. The specimen was incubated with rabbit anti-DBC2 antibody before detection with mouse anti-rabbit antibody conjugated with TRITC. A counter stain of nuclei with DAPI is shown in the right. This figure demonstrates expression of endogenous DBC2 in 293 cells and effective knockdown of DBC2 by RNAi.

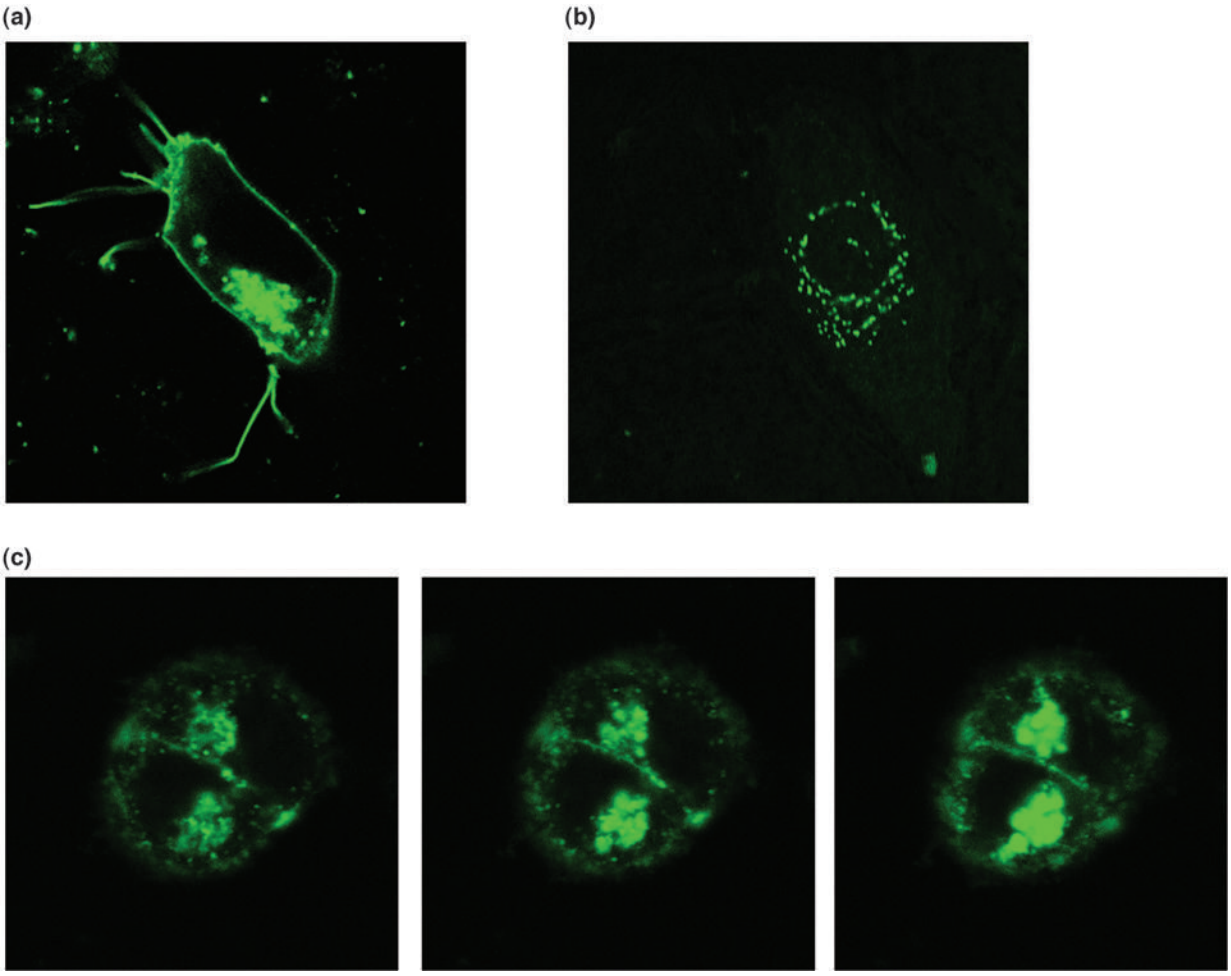


**Figure 3.**

*(a)*. VSVG-GFP signal in wild type 293 cells was observed at the cellular membrane and the Golgi apparatus. *(b)*. VSVG-GFP distribution during incubation at 39 °C is shown. VSVG-GFP remained at the ER, illustrating disruption of VSVG-GFP export from the ER. *(c)*. VSVG-GFP movement was recorded by taking movies after lowering the incubation temperature from 39 °C to 32 °C. Still frames from the movies demonstrated the increase of signal intensity at the Golgi apparatus as time passed, indicating the accumulation of VSVG-GFP at the area. The middle frame was recorded 2.5 minutes after the left frame and the right frame was recorded 5.1 minutes after the left frame.

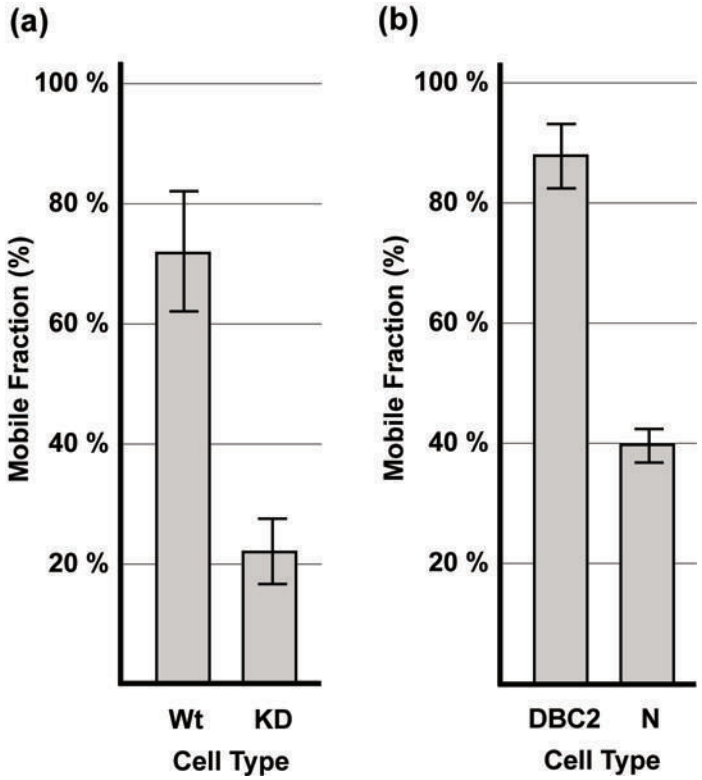


**Figure 4.**

Mobile fractions (MF) are demonstrated in the figure. Error bars indicate the standard deviation. (a) MF of VSVG is shown. “Wt” and “KD” represent VSVG-GFP MF in wild type 293 cells and in 293 cells with DBC2 knockdown, respectively. MF dropped from 72 % (±10%) to 22% (±6%). (b) MF of DBC2 is shown. “DBC2” and “N” represent GFP-DBC2 MF in wild type 293 cells with and without nocodazole treatment. DBC2 MF was 88% (±5%) in wild type cells while 40 % (±3%) in nocodazole treated cells.

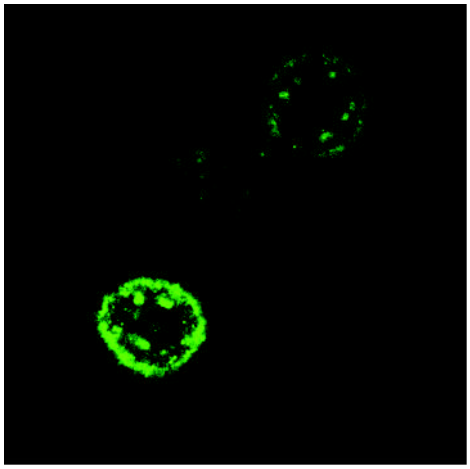

**Figure 5.**
DBC2 was knocked down with RNAi in 293 cells. The distribution of VSVG-GFP was different from that of Figure 3A, since there was an absence of signal at the Golgi complex, an addition of signal in the cytoplasm and a rugged distribution of VSVG-GFP at the cellular membrane. This abnormal distribution pattern may be ascribed to the improper processing of VSVG-GFP at the Golgi.

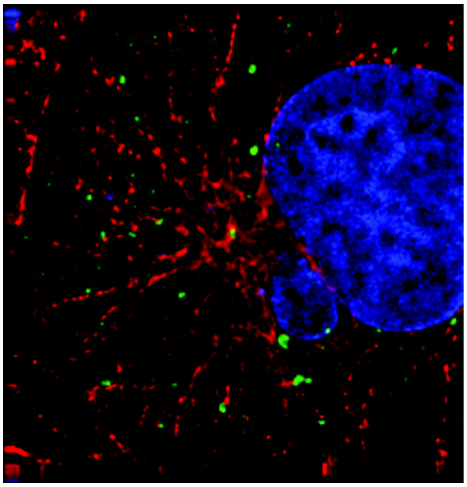

**Figure 6.**
Subcellular localization of DBC2 and tublin is shown. When GFP-DBC2-GFP was expressed at a low level, it appeared near the microtubule network (red in the figure).